Published in final edited form as:
Dev Neurobiol. 2008 September 1; 68(10): 1243–1256. doi:10.1002/dneu.20650.

Efficient co-packaging and co-transport yields post-synaptic co-localization of neuromodulators associated with synaptic plasticity

J. E. Lochner[1,2], **E. Spangler**[3,4], **M. Chavarha**[1], **C. Jacobs**[2], **K. McAllister**[2], **L. C. Schuttner**[4], and **B. A. Scalettar**[5]

[1]Department of Chemistry, Lewis & Clark College, Portland, OR 97219

[2]Department of Biochemistry and Molecular Biology, Lewis & Clark College, Portland, OR 97219

[3]Department of Biology, Lewis & Clark College, Portland, OR 97219

[4]Department of Psychology, Lewis & Clark College, Portland, OR 97219

[5]Department Physics, Lewis & Clark College, Portland, OR 97219

Abstract

Recent data suggest that tissue plasminogen activator (tPA) influences long-term plasticity at hippocampal synapses by converting plasminogen into plasmin, which then generates mature brain-derived neurotrophic factor (mBDNF) from its precursor, proBDNF. Motivated by this hypothesis, we used fluorescent chimeras, expressed in hippocampal neurons, to elucidate (*1*) mechanisms underlying plasminogen secretion from hippocampal neurons, (*2*) if tPA, plasminogen, and proBDNF are co-packaged and co-transported in hippocampal neurons, especially within dendritic spines, and (*3*) mechanisms mediating the transport of these neuromodulators to sites of release. We find that plasminogen chimeras traffic through the regulated secretory pathway of hippocampal neurons in dense-core granules (DCGs) and that tPA, plasminogen, and proBDNF chimeras are extensively co-packaged in DCGs throughout hippocampal neurons. We also find that 80% of spines that contain DCGs contain chimeras of these neuromodulators in the same DCG. Finally, we demonstrate, for the first time, that neuromodulators undergo co-transport along dendrites in rapidly mobile DCGs, indicating that neuromodulators can be efficiently recruited into active spines. These results support the hypothesis that tPA mediates synaptic activation of BDNF by demonstrating that tPA, plasminogen, and proBDNF co-localize in DCGs in spines, where these neuromodulators can undergo activity-dependent release and then interact and/or mediate changes that influence synaptic efficacy. The results also raise the possibility that frequency-dependent changes in extents of neuromodulator release from DCGs influence the direction of plasticity at hippocampal synapses by altering the relative proportions of two proteins, mBDNF and proBDNF, that exert opposing effects on synaptic efficacy.

Keywords

tPA; BDNF; plasminogen; synaptic plasticity; hippocampus

Address correspondence to Bethe Scalettar, Department of Physics, Lewis & Clark College, Portland, OR 97219. Tel: 503−768−7585; Fax: 503−768−7369; E-mail: bethe@lclark.edu.

INTRODUCTION

Long-term memory formation is accompanied by enduring changes in synaptic efficacy, which are triggered in part by the secretion, and subsequent activity, of neuromodulators. Brain-derived neurotrophic factor (BDNF) and tissue plasminogen activator (tPA) are two neuromodulators that are highly expressed in the hippocampus and that are implicated in modifying synaptic efficacy during learning and memory. For example, mature BDNF (mBDNF) induces processes that underlie long-term potentiation (LTP), including stimulating the growth of post-synaptic dendritic spines, augmenting synapse density, and eliciting long-lasting enhancement of synaptic transmission (Lessmann et al., 1994; Levine et al., 1995; Li et al., 1998; Tyler and Pozzo-Miller, 2001; Tyler and Pozzo-Miller, 2003). In contrast, precursor BDNF (proBDNF) induces processes that underlie long-term depression (LTD), such as spine retraction, that weaken synaptic connections (Lu et al., 2005; Woo et al., 2005; Zagrebelsky et al., 2005).

Recent data suggest that tPA influences synaptic plasticity by activating BDNF. Specifically, electrophysiological and biochemical data obtained in studies of hippocampal neurons provide support for the hypothesis that secreted tPA first converts plasminogen into the active protease plasmin, and plasmin then converts extracellular proBDNF into mBDNF (Pang et al., 2004); see Fig. 1. Intriguingly, this mechanism suggests that interactions between tPA, plasminogen, and proBDNF could influence the direction of plasticity at hippocampal synapses by controlling the relative proportions of two proteins, mBDNF and proBDNF, that exert opposing (enhancing and inhibiting) effects on synaptic efficacy (Lu et al., 2005).

Although supported by a body of compelling data, key assumptions and implications of the model in Fig. 1 remain unproven. For example, the model assumes that tPA, plasminogen, and proBDNF are strategically positioned to interact at hippocampal synapses. However, synaptic co-localization of tPA, plasminogen, and proBDNF has not previously been observed (Pang et al., 2004). In addition, the model suggests that synaptic stimulation that induces LTP will lead to a synaptic accumulation of mBDNF (relative to the precursor), whereas stimulation that induces LTD will lead to an accumulation of proBDNF. However, the processes that lead to the synaptic secretion and activation of proBDNF in response to different electrical stimuli remain elusive.

Motivated by this hypothesized mechanism, and associated recent interest in possible interactions between tPA, plasminogen, and proBDNF, we have studied (at the individual organelle level) the packaging, transport, and secretory trafficking of these proteins simultaneously in cultured hippocampal neurons. We also have studied plasminogen individually, because plasminogen is synthesized by neurons in the hippocampus, but hippocampal plasminogen is relatively poorly understood (Tsirka et al., 1997; Basham and Seeds, 2001).

To facilitate our studies, we have constructed DNAs encoding several fluorescent chimeric proteins, including tPA-enhanced green fluorescent protein (tPA-EGFP), proBDNF-mCherry, and plasminogen-mCherry, and we have effectively expressed these chimeras in hippocampal neurons, including mature neurons. To date, we have used our chimeras, in conjunction with wide-field fluorescence microscopy and total internal reflection fluorescence microscopy (TIRFM), to elucidate (*1*) mechanisms underlying plasminogen secretion from hippocampal neurons, (*2*) if tPA, plasminogen, and proBDNF are packaged and transported to release sites within the same, or different, organelles, (*3*) if these neuromodulators co-localize at the organelle level in post-synaptic dendritic spines, and (*4*) mechanisms mediating the organelle-based transport of these neuromodulators to sites of

release in mature neurons. We find 82 − 89% co-localization of puncta containing plasminogen chimeras with markers for dense-core granules (DCGs), indicating that secretion of plasminogen from hippocampal neurons is regulated. In addition, we find extensive co-localization of tPA, plasminogen, and proBDNF chimeras within DCGs of hippocampal neurons, revealing efficient co-packaging. We also find that 80% of spines that contain DCGs contain chimeras of these neuromodulators in the same DCG. Finally, we find a large pool of rapidly mobile DCGs containing the chimeras in dendrites and near the plasma membrane, indicating that tPA, plasminogen, and proBDNF can be efficiently recruited to sites of release, particularly into active spines. These results demonstrate that plasminogen, like tPA and proBDNF, traffics through the regulated secretory pathway of hippocampal neurons. The results also provide data in support of the hypothesis that tPA mediates extracellular activation of BDNF by demonstrating that hippocampal neurons produce a pool of DCGs containing tPA, plasminogen, and proBDNF at post-synaptic sites, where these neuromodulators can undergo activity-dependent release from DCGs and then interact and/or mediate changes that influence learning and memory.

METHODS

Cell culture

Hippocampal neurons from 18-day-old embryonic rats were cultured on 18-mm diameter round glass #1 cover slips, as described previously (Goslin and Banker, 1998).

Transfection and electroporation

Expression vectors, including those encoding tPA-EGFP, proBDNF-mCherry, proBDNF-EGFP, plasminogen-mCherry, and Azurite (Mena et al., 2006) were constructed using standard subcloning techniques. Proteins synthesized from the proBDNF vectors should remain largely in the precursor form during intracellular trafficking, because BDNF is secreted primarily in its “pro” form (Mowla et al., 1999; Mowla et al., 2001; Chen et al., 2004; Lu et al., 2005).

Two methods were used to introduce these (and similar) vectors into hippocampal neurons. In some cases, vectors were introduced into hippocampal neurons using Lipofectamine 2000 (Ohki et al., 2001), following a protocol optimized for transfection of mature neurons (Sharma et al., 2006). In brief, hippocampal neurons were cultured on cover slips at 150,000 or 300,000 cells per 60 mm culture dish until the cells were 14 − 15 DIV (days in vitro). In preparation for transfection, 1.0 − 3.0 μg of DNA was diluted into 50 μl of pre-warmed minimal essential medium (MEM), and this solution was vortexed for 1 s. In addition, 1.0 − 3.0 μl of Lipofectamine 2000 was diluted into a separate 50 μl volume of pre-warmed MEM, and this solution also was vortexed for 1 s. The dilute Lipofectamine was added to the dilute DNA, gently vortexed for 2 s, and incubated for 20 min. Cover slips were then transferred to transfection plates containing 3 ml pre-warmed, CO_2 equilibrated MEM and 100 μM R-2-amino-5-phosphonopentanoate (APV), a selective N-methyl d-aspartate receptor antagonist. 400 μl of equilibrated MEM was added to the Lipofectamine 2000/DNA solution, and the 500-μl lipid/DNA/MEM solution was pipetted directly onto cover slips. The cells were incubated for 3.5 hours at 37°C in 5% CO_2. During incubation, the original culture medium was again supplemented with 100 μM APV. Cover slips were returned to the original culture dish, and neurons were allowed to express the transfected genes for a minimum of 20 hours.

In other cases, vectors were introduced into freshly isolated hippocampal neurons using electroporation, following Amaxa's instruction for the rat nucleofector kit (Amaxa,

Gaithersburg, MD). The neurons then were allowed to express the electroporated genes for times ranging from a few days to several weeks before imaging.

Staining

Staining was used to visualize overall neuronal morphology and especially to delineate spines. In experiments using fixed hippocampal neurons, actin filaments, which are abundant in spines and growth cones, were stained using FITC- or Alexa 350-conjugated phalloidin (Invitrogen, Eugene, OR).

In addition, immunostaining was used to detect endogenous neuromodulators in hippocampal neurons. To detect endogenous tPA, we affinity purified a goat anti-tPA antibody (Millipore, Billerica, MA), following a protocol provided by Dr. David Wells (Yale University). To detect endogenous proBDNF, we used a sheep anti-BDNF antibody (Millipore) that has been reported in the literature to detect endogenous BDNF in hippocampal neurons (Swanwick et al., 2004). These primary antibodies were labeled with donkey anti-goat Cy3 and donkey anti-sheep Alexa 594 antibodies, respectively (Invitrogen).

Imaging

Multi-color wide-field imaging of fixed neurons was used to study protein distribution throughout cells. Wide-field images of fixed cells were collected on either a Leica microscope (Leica Microsystems, Chantilly, VA) under the control of Metamorph software (Universal Imaging, Downington, PA) or on an Olympus microscope (Olympus, Lake Success, NY) under the control of DeltaVision software (Applied Precision, Issaquah, WA).

Dual-color wide-field and TIRFM imaging of living neurons were used to study the trafficking of DCGs containing chimeras near sites of release. Dual-color images of living cells were collected using a fluorescence microscopy system that includes a multi-line krypton-argon laser, an acousto-optic tunable filter that facilitates rapid wavelength switching, and an Optical Insights dual-view beam splitter that facilitates simultaneous dual-color image acquisition (Roper Scientific, Tucson, AZ). The system also includes a very high (1.45) NA objective. This objective can be used for TIRFM imaging if the laser light is directed into the very periphery of the objective, and it can be used for wide-field imaging if the laser light is directed through more central parts of the objective. In the case of TIRFM imaging, the peripherally directed laser light leads to excitation light that decays exponentially in intensity along the direction perpendicular to the glass/liquid interface to which the cells adhere (Axelrod, 2003). This exponentially decaying excitation light causes fluorophores to appear progressively dimmer as they move away from the interface. Moreover, fluorophores are virtually invisible when they are more than ~300 nm from the interface, and thus from the plasma membrane (Johns et al., 2001; Silverman et al., 2005).

Methodology for mounting samples depended on whether the neurons were live or fixed. In the case of live imaging, cover slips containing hippocampal neurons were mounted in a chamber in Hanks-based imaging medium augmented with 10 mM HEPES and 0.6% glucose. The chamber was maintained at 32°C. For fixed imaging, cover slips containing neurons were mounted in elvanol and sealed to a slide with clear nail polish.

Methodology for acquiring images also depended on whether the neurons were live or fixed. Time-lapse images of DCG transport in living cells were generated by taking images of the same focal plane every 100 − 200 ms and either imaging both emission wavelengths simultaneously using the dual-view beam splitter or imaging the two emission wavelengths separately with rapid switching. Most static images of distribution in fixed cells were generated by optically sectioning cells in 0.2 μm focal increments (Hiraoka et al., 1991;

Scalettar et al., 1996); these images were deblurred using a constrained iterative deconvolution algorithm (Scalettar et al., 1996) to improve image clarity.

Data analysis

Co-localization—We determined the percentage of puncta containing plasminogen-mCherry that overlap with DCGs by separately imaging the distribution of plasminogen-mCherry and proBDNF-EGFP in a fixed, dual-labeled cell; this was accomplished using standard filters that isolate the fluorescence from each labeled species. The individual grayscale images revealing the distribution of each labeled species were colored red or green to reflect the emission from the two labels and superimposed to produce dual-color images that reveal overlap in protein distribution. Using these dual-color images, we quantified the percent overlap between puncta containing plasminogen-mCherry and puncta containing proBDNF-EGFP by counting yellow puncta in one optical section in a sub-region of a cell and normalizing the number of yellow puncta by the total number of red and yellow puncta in that sub-region. In quantifying overlap, we neglected slight (< 0.1 μm) lack of registration in the center positions of overlapping puncta, because wavelength-dependent image shifts are known to cause such slight registration problems in multi-color images (Hiraoka et al., 1991; Scalettar et al., 1996). Other co-localization data were analyzed similarly.

Tracking—DCGs were tracked laterally in two dimensions (*x*,*y*) in background-subtracted movies using the public domain program ImageJ. Tracking involved manually surrounding a DCG in a given frame with an appropriate (usually circular) shape and calculating the center of mass of the fluorescence distribution in the shape using ImageJ. Tracking of a DCG in successive frames was continued as long as the DCG could be identified unambiguously.

Quantification of speeds and diffusion coefficients—Lateral DCG motion was characterized quantitatively by computing the mean-squared displacement, $\langle r^2 \rangle$, of DCGs as a function of time, *t*, and fitting to a model that describes “diffusive” and “directed” motion as follows (Saxton and Jacobson, 1997; Abney et al., 1999):

$$\langle r^2 \rangle = 4Dt + v^2 t^2 \quad (1)$$

Here, *r* is displacement, *D* is the diffusion coefficient, and *v* is speed; brackets <> denote averaging, which was performed as described previously (Abney et al., 1999). In Eq. 1, diffusive motion produces a linear relationship between $\langle r^2 \rangle$ and *t*, whereas directed motion produces a linear relationship between $\langle r^2 \rangle^{1/2}$ and *t*. *D*'s and *v*'s were computed from fits to Eq. 1, as described previously (Abney et al., 1999).

Quantification of data statistics—Statistical data are reported as a mean ± standard deviation. Statistical similarities and differences between data were analyzed using the Student's t-test function in Excel and are reported in terms of “p” values (Microsoft, Redmond, WA). For the t-test analysis, we adopted standard criteria and assumed that two data sets are statistically different if $p < 0.05$ and are statistically similar if $p > 0.05$.

RESULTS

Plasminogen-chimeras localize to DCGs in hippocampal neurons

Plasminogen has emerged as a key player in learning, memory, and neurodegeneration in the hippocampus, and yet little is known about its localization or secretory trafficking in hippocampal neurons. To address these issues, we first visualized the distribution of a plasminogen-mCherry chimera in hippocampal neurons. Fig. 2A shows the soma and

proximal processes of a fixed 7-DIV hippocampal neuron expressing plasminogen-mCherry and the photostable blue fluorescent protein, Azurite, which delineates overall neuronal morphology. The chimera localizes to regions of the soma typically occupied by the Golgi and to spherical organelles that are distributed throughout the soma and processes, suggesting that plasminogen traffics through the secretory pathway of hippocampal neurons. Fig. 2B shows a growth cone from a fixed 7-DIV hippocampal neuron expressing plasminogen-mCherry and Azurite. This image illustrates that plasminogen-mCherry often also accumulates in growth cones of developing neurons.

We next determined the identity of the organelles that house plasminogen. To this end, we expressed plasminogen-mCherry and proBDNF-EGFP (an established marker for DCGs) (Haubensak et al., 1998; Hartmann et al., 2001; Brigadski et al., 2005; Kolarow et al., 2007) in hippocampal neurons, and we generated dual-color wide-field fluorescence images that reveal the degree of co-localization between the two chimeras. Fig. 2C shows part of a process from a fixed 4-DIV hippocampal neuron expressing plasminogen-mCherry and proBDNF-EGFP. The two proteins co-localize extensively in puncta, as demonstrated by the dominance of yellow in the image. Similar co-localization data also were obtained in neurons of greater maturity and with different levels of neuromodulator expression. Quantification revealed that 82 ± 6% of plasminogen-mCherry-containing puncta overlap with proBDNF-EGFP-containing puncta (n = 3 cells, 625 puncta). Quantification also revealed that 87 ± 4% of proBDNF-EGFP-containing puncta overlap with plasminogen-mCherry-containing puncta (n = 3 cells, 562 puncta). These degrees of co-localization are comparable to, or significantly better than, those commonly obtained in co-localization studies directed at proving that a protein localizes to DCGs; for example, co-localization between cyan and yellow chimeras of the DCG proteins tPA and proneuropeptide Y in hippocampal neurons is ~88%, and co-localization between chimeras of chromogranin B and the endogenous DCG protein dopamine-beta-hydroxylase in PC12 cells is ~65% (Lang et al., 1997; Silverman et al., 2005). Thus, our co-localization data for plasminogen-mCherry strongly suggest that plasminogen is housed in DCGs and traffics predominantly through the regulated secretory pathway of hippocampal neurons.

We also expressed plasminogen-mCherry and tPA-EGFP (another established marker for DCGs) (Lochner et al., 1998; Silverman et al., 2005) in hippocampal neurons and assayed for co-localization of these two chimeras. We observed fewer cells co-expressing plasminogen-mCherry and tPA-EGFP than cells co-expressing plasminogen-mCherry and proBDNF-EGFP. However, in cells co-expressing the former two proteins, co-localization was high. Fig. 2D shows parts of processes from a fixed 2-DIV hippocampal neuron expressing plasminogen-mCherry and tPA-EGFP. The two proteins again co-localize extensively in puncta, as demonstrated by the dominance of yellow in the image. Quantification revealed that 89 ± 5% of plasminogen-mCherry-containing puncta overlap with tPA-EGFP-containing puncta and that 88 ± 6% of tPA-EGFP-containing puncta overlap with plasminogen-mCherry-containing puncta (n = 3 cells, 423 puncta).

tPA, plasminogen, and proBDNF chimeras co-localize, and undergo co-transport, in DCGs in hippocampal neurons

The data in Fig. 2C,D demonstrate that plasminogen and proBDNF, and plasminogen and tPA, are co-packaged in DCGs of fixed hippocampal neurons. We also attempted to obtain triple co-localization data using three spectrally compatible chimeras of tPA, proBDNF, and plasminogen, but this approach generally yielded poor expression. Thus, here we have addressed co-localization of chimeras of the three neuromodulators pair-wise (using doubly expressing neurons). Fig. 3 demonstrates co-packaging of the final pair, tPA-EGFP and proBDNF-mCherry, in a fixed 8-DIV hippocampal neuron. Quantification revealed that 89 ± 5% of tPA-EGFP-containing puncta overlap with proBDNF-mCherry-containing puncta (n

= 3 cells, 1117 puncta) and that 92 ± 8% of proBDNF-mCherry-containing puncta overlap with tPA-EGFP-containing puncta (n = 3 cells, 1732 puncta). These degrees of co-localization are statistically indistinguishable from degrees of co-localization between plasminogen-mCherry and proBDNF-EGFP chimeras. For example, statistical comparison of tPA overlap with proBDNF to plasminogen overlap with proBDNF yields $p = 0.18$ (> 0.05; Student's t-test). The extensive pair-wise co-localization of tPA and proBDNF, of plasminogen and proBDNF, and of plasminogen and tPA, together with the statistical similarity of these pair-wise co-localizations, demonstrates that all three neuromodulators are co-packaged in DCGs in hippocampal neurons.

We also assayed for neuromodulator co-transport in living neurons, which could facilitate pivotal processes, such as tPA-mediated activation of proBDNF in the extracellular space at synapses. Study of co-transport in living neurons also allowed us to determine important transport parameters, as discussed in the last section of RESULTS, and it served as a control for overlap that is generated by diffraction by revealing overlap that persists as DCGs move.

Fig. 4A demonstrates co-packaging of tPA-EGFP and proBDNF-mCherry in a living 18-DIV hippocampal neuron. The two proteins again co-localize extensively in puncta of this living neuron, as demonstrated by the dominance of yellow in the overlay. Moreover, this co-localization persists in mobile puncta, demonstrating neuromodulator co-transport. This can be seen by examining the associated movie, which is provided as supplemental data. Fig. 4B also reveals neuromodulator co-transport quantitatively, demonstrating close parallels in displacement versus time plots obtained by separately tracking red and green signals for the two puncta identified with arrows in Fig. 4A.

tPA, plasminogen, and proBDNF chimeras co-localize in DCGs in dendritic spines

The tPA/plasmin system and proBDNF are hypothesized to interact at synapses (Zhuo et al., 2000; Pang et al., 2004). Moreover, many processes mediated by tPA, plasminogen, proBDNF, and mBDNF, such as those underlying LTP and LTD, are believed to take place on the post-synaptic side of synapses (reviewed in (Massey and Bashir, 2007; Raymond, 2007)). In light of this, we determined if tPA, plasminogen, and proBDNF chimeras localize to, and co-localize in, DCGs in post-synaptic dendritic spines of mature hippocampal neurons. To this end, we stained fixed, singly and doubly expressing neurons with fluorescently conjugated phalloidin. Stained phalloidin reveals neuronal morphology, notably dendritic spine morphology, because actin is abundant in spines (Kaech et al., 1997).

We have shown previously that tPA chimeras localize to individual DCGs in spines (Lochner et al., 2006). Vesicle clusters containing proBDNF chimeras also have been found to co-localize with postsynaptic density protein-95-DsRed, a fluorescent chimera used as a postsynaptic marker of glutamatergic synapses (Kolarow et al., 2007). However, individual synaptically localized DCGs containing proBDNF have not been studied previously. Little past work has been directed at elucidating plasminogen localization within synapses of hippocampal neurons.

In light of these unresolved issues, we first extended our past work and demonstrated that proBDNF and plasminogen chimeras also localize to individual DCGs in spines of hippocampal neurons. Fig. 5A shows a dendritic process and spines stained with FITC-conjugated phalloidin. Three of these spines have DCGs containing proBDNF-mCherry. Fig. 5B shows another dendritic process and set of spines stained with FITC-conjugated phalloidin. In this case, two spines have DCGs containing plasminogen-mCherry.

We next demonstrated that tPA, proBDNF, and plasminogen co-localize extensively in individual DCGs in spines. Fig. 5C shows a dendritic process and spines stained with

Alexa-350-conjugated phalloidin, which fluoresces blue. This image shows that DCGs containing both tPA and proBDNF chimeras are present in many dendritic spines of mature hippocampal neurons. Similarly, Fig. 5D shows that DCGs containing both plasminogen and proBDNF chimeras are present in dendritic spines of mature hippocampal neurons. Quantification revealed that 27 ± 9% of spines (n = 8 cells, 203 spines) contain at least one DCG containing co-localizing chimeras. In addition, 80 ± 18% of the spines that contained at least one DCG contained co-localizing chimeras of neuromodulators in the same DCG. This degree of co-localization is statistically indistinguishable from co-localization in all sub-domains of neurons. For example, statistical comparison of tPA overlap with proBDNF in all sub-domains to overlap in spines yields $p = 0.20$ (> 0.05; Student's t-test).

Chimeric and endogenous neuromodulators exhibit similar attributes

Unlike transport, localization of neuromodulators to neuronal sub-domains like spines and growth cones can also be studied by using immunofluorescence to visualize the distribution of endogenous proteins in fixed cells. When possible, we also used immunofluorescence to map distribution, because the endogenous neuromodulators are our real interest. Immunofluorescence studies also allowed us to confirm that our chimeras mimic their endogenous analogs. Fig. 6 shows examples of our immunofluorescence data, revealing that endogenous proBDNF localizes to growth cones and to spines in spherical organelles, similar to our chimera. Our immunofluorescence images also reveal that endogenous tPA localizes to growth cones and to spines, and our images, and analogous images presented in the literature (Shin et al., 2004;Swanwick et al., 2004), reveal that endogenous tPA and endogenous proBDNF produce a punctate distribution pattern in the cell body and processes that is similar to the distribution pattern produced by our chimeras.

Our past work and past work from other laboratories also demonstrate that our chimeras mimic their endogenous analogs by demonstrating that tPA and proBDNF chimeras co-localize with endogenous secretogranin II, another established marker for DCGs (Rosa et al., 1985; Schwarzer et al., 1997; Farhadi et al., 2000), in hippocampal neurons, and that these chimeras undergo stimulus/calcium-dependent secretion from post-synaptic sites of hippocampal neurons (Hartmann et al., 2001; Brigadski et al., 2005; Silverman et al., 2005; Lochner et al., 2006; Kolarow et al., 2007). These attributes of the chimeras are consistent with established attributes of endogenous tPA and proBDNF in hippocampal neurons, particularly their stimulus/calcium-dependent secretion (Baranes et al., 1998; Balkowiec and Katz, 2002; Pang et al., 2004). Similarly, the presence of our plasminogen chimera in the regulated secretory pathway of rat hippocampal neurons is consistent with the presence of endogenous plasminogen in the regulated secretory pathway of cells in the rat cerebral cortex (Bruno and Cuello, 2006).

A large pool of mobile DCGs containing neuromodulators is present near sites of release

Current models hypothesize that the neuromodulators tPA, plasminogen, and proBDNF are present at active spines to initiate changes such as those underlying learning and memory (Pang et al., 2004). However, our current work shows that many spines in unstimulated hippocampal neurons do not house DCGs containing tPA, plasminogen, and proBDNF. If one of these “empty” spines becomes active, a DCG needs to be recruited. Thus, it is of interest to elucidate how rapidly DCGs containing tPA, plasminogen, and proBDNF can be recruited into spines, and to the plasma membrane, during periods of activity.

One potentially important determinant of this time-scale is the dynamics of DCGs that house tPA, plasminogen, and proBDNF (Silverman et al., 2005). To address this poorly understood issue, we determined mechanisms and rates of transport of DCGs containing these neuromodulators using hippocampal neurons that co-express spectrally compatible

chimeras. Wide-field and TIRFM movies of such cells both reveal that many DCGs containing neuromodulators near spines and near the plasma membrane undergo rapid lateral trafficking. Fig. 7A shows time-lapse, dual-color images of the distribution of DCGs containing tPA-EGFP and proBDNF-mCherry in part of a process of a living 8-DIV hippocampal neuron. Here, green indicates DCG positions at an initial time, red indicates DCG positions at a specified later time, and yellow indicates overlap of green and red. DCGs overlap completely when the time interval between successive pictures is 0 s, and this overlap is lost substantially within less than 9 s. These and similar data demonstrate that DCGs containing chimeras of neuromodulators are substantially mobile over a time scale of < 9 s.

We also determined rates underlying active lateral transport of DCGs containing neuromodulators near sites of release. To this end, we tracked DCGs and generated plots of $\langle r^2 \rangle^{1/2}$ versus *t*. Fig. 7B shows several representative plots obtained by tracking DCGs in Panel A. The plots are linear, implying that the trafficking was directed, and their slopes give speeds on the order of one μm/s, revealing that trafficking was rapid. Additional tracking and quantification revealed that DCGs in dendrites and near the plasma membrane undergo rapid and directed lateral transport at an average speed of 0.87 ± 0.54 μm/s (n = 4 cells, 103 DCGs).

Our TIRFM movies also reveal that many membrane-proximal DCGs containing neuromodulators undergo rapid, axial trafficking near the plasma membrane. Axial mobility is especially important, because it mediates delivery of DCGs to the plasma membrane as a prelude to release. The extensive axial mobility of DCGs containing neuromodulators is exemplified by the fact that our TIRFM movies reveal substantial flicker, which arises when DCGs move axially and are exposed to different intensities of excitation light at different depths from the plasma membrane. Fig. 7C shows some representative images of intensity flicker from a dual-labeled DCG.

DISCUSSION

The experiments described here were directed at determining (*1*) mechanisms underlying plasminogen secretion from hippocampal neurons, (*2*) if tPA, plasminogen, and proBDNF are packaged and transported to release sites within the same, or different, organelles, (*3*) if these neuromodulators co-localize at the organelle level in post-synaptic dendritic spines, and (*4*) mechanisms mediating the organelle-based transport of these neuromodulators to sites of release in mature neurons. Here we discuss these issues, as well as how our data bear on current models of the function of tPA, plasminogen, and BDNF in learning and memory.

Implications for plasminogen localization and secretion from hippocampal neurons

Many key issues surrounding plasminogen localization and trafficking in hippocampal neurons remain unresolved. These include identifying domains of localization within hippocampal neurons and determining mechanisms underlying secretion and transport. Several lines of evidence do, however, provide compelling evidence that hippocampal neurons synthesize plasminogen. For example, plasminogen mRNA has been detected in hippocampal neurons, and plasminogen immunoreactivity has been detected at relatively low resolution in images of the mouse hippocampus (Tsirka et al., 1997; Basham and Seeds, 2001; Salles and Strickland, 2002). In addition, plasminogen expression is strongly induced in the rat hippocampus in response to injection of kainic acid, which destroys pyramidal cells in the hippocampus and leads to neurodegeneration (Matsuoka et al., 1998).

Here we have addressed some of the unresolved issues surrounding hippocampal plasminogen using a plasminogen chimera, because the chimera facilitates study of living

neurons and is easier to detect than the endogenous protein. Our data reveal that organelles containing plasminogen also contain tPA and proBDNF, and that organelles containing plasminogen often accumulate in growth cones of developing hippocampal neurons and are present in spines of mature neurons. Co-localization with the DCG markers tPA and proBDNF strongly indicates that plasminogen is housed in DCGs. A growth-cone biased distribution pattern in developing cells further supports the idea that plasminogen is housed in DCGs, because DCGs in PC-12 and AtT-20 cells exhibit a growth-cone biased distribution (Burke et al., 1997; Lang et al., 1997; Lochner et al., 1998). To our knowledge, localization of plasminogen to DCGs in hippocampal neurons, or in any other cell type, has not been demonstrated previously. Localization to spines also has not been demonstrated previously and provides further support for the idea that plasminogen plays a role in learning and memory in the hippocampus.

Our data also strongly indicate that plasminogen undergoes regulated release from hippocampal neurons, because we find that plasminogen is present in an organelle that undergoes regulated exocytosis (Burgoyne and Morgan, 2003). The mode of plasminogen release from hippocampal neurons has not been determined previously and is important to elucidate, because plasminogen secretory trafficking varies with cell type. Plasminogen is constitutively released from liver cells, which lack a regulated secretory pathway (Hay and Martin, 1992). In contrast, plasminogen appears to undergo regulated release from cells in the rat cerebral cortex and in the human central nervous system (Teesalu et al., 2002; Bruno and Cuello, 2006).

Implications for hypotheses about tPA/plasmin-mediated activation of proBDNF

Data obtained recently provide support for the hypothesis that tPA influences long-term hippocampal plasticity by converting plasminogen to plasmin, which then cleaves proBDNF to produce mBDNF; see Fig. 1. mBDNF then can induce changes that influence LTP, whereas proBDNF can induce changes that influence LTD (Pang et al., 2004;Woo et al., 2005). Specifically, these data reveal that plasmin, or the tPA/plasminogen system, but not tPA alone, can cleave proBDNF *in vitro*. More compellingly, these data also reveal deficits in late LTP in slices from the hippocampus of mice deficient for tPA, plasminogen, or BDNF, and a pattern of deficit rescue upon application of these proteins that supports the model in Fig. 1.

Despite these suggestive data, several key tenets of the model in Fig. 1 remain unproven. Specifically, synaptic co-localization of tPA, plasminogen, and proBDNF has not previously been demonstrated (Pang et al., 2004). Some of the interactions in the model also would be facilitated by activity-dependent co-release of tPA, plasminogen, and proBDNF from synaptic structures. However, activity-dependent co-release, like co-localization, has not previously been demonstrated.

To begin to address these, and related, issues, we co-expressed fluorescent chimeras of tPA, plasminogen, and proBDNF in mature hippocampal neurons. Using this approach, we demonstrated that tPA, plasminogen, and proBDNF are extensively co-packaged, and rapidly co-transported, in DCGs in the soma and along processes of mature hippocampal neurons. We also demonstrated that tPA, plasminogen, and proBDNF co-localize in individual DCGs at synapses, particularly in dendritic spines, of mature hippocampal neurons. This latter result provides direct confirmation of a hypothesis about tPA, plasminogen, and proBDNF localization embodied in the model in Fig. 1, revealing that these proteins are strategically positioned to undergo release at spines where they can participate in the hypothesized activation cascade. This result also provides confirmation that release will be activity-dependent, because DCG exocytosis is highly suppressed in the absence of activity (Burgoyne and Morgan, 2003;Fulop et al., 2005).

Implications for intracellular interaction of neuromodulators

Our data reveal that the neuromodulators tPA, plasminogen, and proBDNF co-localize in DCGs in rat hippocampal neurons. This result raises the possibility of intracellular interaction of these neuromodulators, which could lead, in turn, to intracellular activation of plasminogen and proBDNF and subsequent secretion of both proteins in their mature form. This possibility has important implications for the model presented in Fig. 1, which postulates that BDNF is secreted in its precursor form and undergoes activation in the extracellular space.

Extensive intracellular interaction of tPA, plasminogen, and proBDNF that leads to significant secretion of the mature form of BDNF is inconsistent with experimental data showing that BDNF is secreted primarily in its precursor form (Mowla et al., 1999; Mowla et al., 2001; Chen et al., 2004; Lu et al., 2005). This suggests that there are mechanisms that limit intracellular interaction of tPA, plasminogen, and proBDNF in rat hippocampal neurons. One possible mechanism, sequestration of tPA, plasminogen, and proBDNF in different vesicles, is inconsistent with our data demonstrating that these proteins co-localize extensively in DCGs of rat hippocampal neurons. A second possible mechanism is control of protein expression (Tsirka et al., 1997). This second mechanism has strong support from data in the literature, which reveal that plasminogen expression is low in rat hippocampal neurons under basal conditions but can be markedly enhanced by stimuli, particularly exposure to kainic acid (Matsuoka et al., 1998). A third possible mechanism is intracellular inhibition of tPA by neuroserpin. This third mechanism is more indirectly supported by data in the literature, which show that neuroserpin is present on DCGs in primary cortical cultured neurons (Ishigami et al., 2007).

Attributes of the co-transport of neuromodulators

We studied the trafficking of DCGs containing tPA, plasminogen, and proBDNF in hippocampal neurons for two primary reasons. First, our spectrum of chimeras allowed us to analyze, for the first time, the trafficking of organelles in neurons that clearly are co-transporting several distinct types of neuromodulators near critical sites of release. Second, trafficking has implications for rates of delivery of tPA, plasminogen, and proBDNF to sites of release, such as spines that lack these pivotal proteins, as discussed in the next section. As such, our data provide unique insight into dynamic events that underlie learning and memory.

We find that DCGs in hippocampal neurons that are near sites of release on the plasma membrane, or that are near (but not within) spines, often undergo rapid, directed trafficking. In contrast, DCGs in chromaffin cells and PC12 cells that are near sites of release on the plasma membrane typically are immobile or undergo very slow, random motion, and DCGs in mature hippocampal neurons typically become immobile once they have entered spines (Burke et al., 1997; Abney et al., 1999; Han et al., 1999; Johns et al., 2001; Ng et al., 2003; Lochner et al., 2006). This atypically fast trafficking of many DCGs in hippocampal neurons may reflect the atypically large distances that DCGs must traverse in these cells to move from sites of synthesis to sites of release. Moreover, the transition to a relatively immobile state once DCGs in mature hippocampal neurons have entered spines may help retain pivotal cargo, like tPA, plasminogen, and proBDNF, at these key sites, thereby facilitating rapid release from spines during times of activity.

Implications for rapid delivery of neuromodulators to spines and other sites of release

Our localization data reveal that the neuromodulators tPA, plasminogen, and proBDNF are co-packaged in DCGs in ~27% of the spines of resting hippocampal neurons. Given this, hippocampal neurons need mechanisms for rapidly and selectively delivering these

neuromodulators to “empty” spines during periods of activity. Our localization and trafficking data suggest one possible way to achieve rapidity: maintenance of a large pool of rapidly mobile DCGs containing neuromodulators along dendritic processes and near the plasma membrane.

To quantify the efficacy of this mechanism, we estimated the average distance between DCGs containing neuromodulators and spines, and we estimated the time for transport to deliver DCGs containing neuromodulators to spines. To address the first (distance scale) issue, we used our images to calculate the dendritic density of DCGs containing neuromodulators. This value varies with expression level, typically ranging from ~0.2 − 0.8 dual-labeled DCGs/μm^2. Importantly, our images of the distribution of endogenous tPA and of endogenous proBDNF in 14 − 18 DIV hippocampal neurons, obtained via immunostaining, and analogous images presented in the literature (Shin et al., 2004; Swanwick et al., 2004) reveal densities of the same order of magnitude, ~0.1 − 0.5 DCGs/μm^2. These densities imply that there will be a DCG containing neuromodulators every few microns along a dendrite of width ~2 μm (Bartlett and Banker, 1984). Thus, DCG/spine separation will be at most a few microns.

To address the second (time scale) issue, we used our transport data and transport theory. The timescale for transport into spines, *t*, can be calculated using the relationship $\langle r^2 \rangle^{1/2} = vt$, where *t* is the time, $\langle r^2 \rangle^{1/2}$ is the distance, and *v* is the speed (Berg, 1993). Using the average DCG speed obtained from our movies, ~0.87 μm/s, and the distance obtained from our density data, at most a few microns, we calculate that *t* will be a few seconds, or less. Consistent with this calculation, we have observed DCGs entering spines within seconds of stimulating hippocampal neurons with high KCl. This suggests that extensive co-packaging along dendrites, together with rapid co-transport, can efficiently supply DCGs containing neuromodulators to spines during periods of activity.

Implications for regulation of the synaptic conversion of proBDNF into mBDNF

Our data reveal that the neuromodulators tPA, plasminogen, and proBDNF co-localize in DCGs in spines. Here we address how this result potentially impacts an important unresolved question surrounding the model in Fig. 1, which is how the extracellular cleavage of proBDNF is influenced by stimulation frequency (Lu et al., 2005).

One hypothesis that has been advanced to answer this question is that high-frequency stimulation induces the secretion of tPA, which leads in turn to the activation of secreted proBDNF and to LTP (Lu et al., 2005). In contrast, low-frequency stimulation does not lead to the secretion of tPA, and this impairs activation of secreted proBDNF and leads to LTD. Frequency-dependent secretion of tPA alone could be achieved by packaging tPA in an organelle with appropriate frequency-dependent exocytotic behavior and by packaging proBDNF in a distinct organelle. However, our co-packaging data suggest that this is not the case, and the data instead suggest that frequency-dependent secretion of tPA alone might be achieved by a frequency-dependent switch in the mechanism of DCG exocytosis at spines.

Recent work indicates that neuroendocrine DCGs (and synaptic vesicles) undergo exocytosis via at least two mechanisms that are distinguished by their extent of organelle-plasma membrane mixing (reviewed in (Ryan, 2003; Scalettar, 2006)). Moreover, the relative prevalence of these mechanisms appears to be influenced by stimulation frequency (Wu, 2004; Fulop et al., 2005; Elhamdani et al., 2006). In the “full-fusion” mechanism, which is prevalent at higher frequencies, the vesicle membrane flattens completely into the plasma membrane. In contrast, in the “incomplete fusion” mechanism, which is prevalent at lower frequencies, the vesicle does not flatten completely into the plasma membrane.

Instead, the vesicle establishes continuity with the extracellular space via a fusion pore, while maintaining some of its integrity and shape.

One important distinction between the complete and incomplete fusion mechanisms is that the latter permits different rates and extents of release of distinct cargo proteins from the same DCG (Holroyd et al., 2002; Taraska et al., 2003; Fulop et al., 2005). This has been demonstrated in neuroendocrine cells, where small proteins like neuropeptide Y are rapidly and completely released from a DCG undergoing incomplete fusion, whereas larger proteins like tPA are slowly and partially released via incomplete fusion (Taraska et al., 2003; Perrais et al., 2004). In light of these data, our synaptic co-packaging data, and the relatively small size of proBDNF, it seems plausible that LTD-inducing stimuli preferentially induce incomplete fusion exocytosis at hippocampal synapses and that this leads to reduced secretion of tPA and to reduced activation of extensively co-secreted proBDNF. In contrast, LTP-inducing stimuli preferentially induce complete fusion exocytosis, and this leads to complete/enhanced release of tPA/plasminogen and to enhanced activation of co-released proBDNF.

Supplementary Material

Refer to Web version on PubMed Central for supplementary material.

Acknowledgments

We thank Dr. Gary Banker, Dr. Stephanie Kaech Petrie, and Barbara Smoody of Oregon Health and Sciences University for advice and for extensive support with the culture of hippocampal neurons, and Dr. James Abney for a critical reading of this manuscript.

Financial Support: This work was supported by National Institutes of Health grants 2 R15 GM061539-02 (to B.A.S.), 2 R15 NS40425-02 (to J.E.L.), and MH 66179 (to Dr. Gary Banker of Oregon Health and Sciences University).

REFERENCES

Abney JR, Meliza CD, Cutler B, Kingma M, Lochner JE, Scalettar BA. Real-time imaging of the dynamics of secretory granules in growth cones. Biophys. J. 1999; 77:2887–2895. [PubMed: 10545386]

Abney JR, Meliza CD, Cutler B, Kingma M, Lochner JE, Scalettar BA. Real-time imaging of the dynamics of secretory granules in growth cones. Biophys J. 1999; 77:2887–2895. [PubMed: 10545386]

Axelrod D. Total internal reflection fluorescence microscopy in cell biology. Methods Enzymol. 2003; 361:1–33. [PubMed: 12624904]

Balkowiec A, Katz DM. Cellular mechanisms regulating activity-dependent release of native brain-derived neurotrophic factor from hippocampal neurons. J Neurosci. 2002; 22:10399–10407. [PubMed: 12451139]

Baranes D, Lederfein D, Huang YY, Chen M, Bailey CH, Kandel ER. Tissue plasminogen activator contributes to the late phase of LTP and to synaptic growth in the hippocampal mossy fiber pathway. Neuron. 1998; 21:813–825. [PubMed: 9808467]

Bartlett WP, Banker GA. An electron microscopic study of the development of axons and dendrites by hippocampal neurons in culture. II. Synaptic relationships. J Neurosci. 1984; 4:1954–1965. [PubMed: 6470763]

Basham ME, Seeds NW. Plasminogen expression in the neonatal and adult mouse brain. J Neurochem. 2001; 77:318–325. [PubMed: 11279287]

Berg, H. Random Walks in Biology. Princeton University Press; Princeton,NJ: 1993. p. 164

Brigadski T, Hartmann M, Lessmann V. Differential vesicular targeting and time course of synaptic secretion of the mammalian neurotrophins. J Neurosci. 2005; 25:7601–7614. [PubMed: 16107647]

Bruno MA, Cuello AC. Activity-dependent release of precursor nerve growth factor, conversion to mature nerve growth factor, and its degradation by a protease cascade. Proc Natl Acad Sci U S A. 2006; 103:6735–6740. [PubMed: 16618925]

Burgoyne RD, Morgan A. Secretory granule exocytosis. Physiol Rev. 2003; 83:581–632. [PubMed: 12663867]

Burke NV, Han W, Li D, Takimoto K, Watkins SC, Levitan ES. Neuronal peptide release is limited by secretory granule mobility. Neuron. 1997; 19:1095–1102. [PubMed: 9390522]

Chen ZY, Patel PD, Sant G, Meng CX, Teng KK, Hempstead BL, Lee FS. Variant brain-derived neurotrophic factor (BDNF) (Met66) alters the intracellular trafficking and activity-dependent secretion of wild-type BDNF in neurosecretory cells and cortical neurons. J Neurosci. 2004; 24:4401–4411. [PubMed: 15128854]

Elhamdani A, Azizi F, Artalejo CR. Double patch clamp reveals that transient fusion (kiss-and-run) is a major mechanism of secretion in calf adrenal chromaffin cells: high calcium shifts the mechanism from kiss-and-run to complete fusion. J Neurosci. 2006; 26:3030–3036. [PubMed: 16540581]

Farhadi HF, Mowla SJ, Petrecca K, Morris SJ, Seidah NG, Murphy RA. Neurotrophin-3 sorts to the constitutive secretory pathway of hippocampal neurons and is diverted to the regulated secretory pathway by coexpression with brain-derived neurotrophic factor. J Neurosci. 2000; 20:4059–4068. [PubMed: 10818141]

Fulop T, Radabaugh S, Smith C. Activity-dependent differential transmitter release in mouse adrenal chromaffin cells. J Neurosci. 2005; 25:7324–7332. [PubMed: 16093382]

Goslin, K.; Banker, G. Rat hippocampal neurons in low-density culture.. In: Banker, G.; Goslin, K.; Banker, G.; Goslin, Ks, editors. Culturing Nerve Cells. MIT Press; Cambridge, MA: 1998. p. 339-370.

Han W, Ng YK, Axelrod D, Levitan ES. Neuropeptide release by efficient recruitment of diffusing cytoplasmic secretory vesicles. Proc Natl Acad Sci U S A. 1999; 96:14577–14582. [PubMed: 10588747]

Hartmann M, Heumann R, Lessmann V. Synaptic secretion of BDNF after high-frequency stimulation of glutamatergic synapses. Embo J. 2001; 20:5887–5897. [PubMed: 11689429]

Haubensak W, Narz F, Heumann R, Lessmann V. BDNF-GFP containing secretory granules are localized in the vicinity of synaptic junctions of cultured cortical neurons. J Cell Sci. 1998; 111:1483–1493. [PubMed: 9580557]

Hay JC, Martin TF. Resolution of regulated secretion into sequential MgATP-dependent and calcium-dependent stages mediated by distinct cytosolic proteins. J Cell Biol. 1992; 119:139–151. [PubMed: 1527165]

Hiraoka Y, Swedlow JR, Paddy MR, Agard DA, Sedat JW. Three-dimensional multiple-wavelength fluorescence microscopy for the structural analysis of biological phenomena. Semin Cell Biol. 1991; 2:153–165. [PubMed: 1720334]

Holroyd P, Lang T, Wenzel D, De Camilli P, Jahn R. Imaging direct, dynamin-dependent recapture of fusing secretory granules on plasma membrane lawns from PC12 cells. Proc Natl Acad Sci U S A. 2002; 99:16806–16811. [PubMed: 12486251]

Ishigami S, Sandkvist M, Tsui F, Moore E, Coleman TA, Lawrence DA. Identification of a novel targeting sequence for regulated secretion in the serine protease inhibitor neuroserpin. Biochem J. 2007; 402:25–34. [PubMed: 17040209]

Johns LM, Levitan ES, Shelden EA, Holz RW, Axelrod D. Restriction of secretory granule motion near the plasma membrane of chromaffin cells. J Cell Biol. 2001; 153:177–190. [PubMed: 11285284]

Kaech S, Fischer M, Doll T, Matus A. Isoform specificity in the relationship of actin to dendritic spines. J Neurosci. 1997; 17:9565–9572. [PubMed: 9391011]

Kolarow R, Brigadski T, Lessmann V. Postsynaptic secretion of BDNF and NT-3 from hippocampal neurons depends on calcium calmodulin kinase II signaling and proceeds via delayed fusion pore opening. J Neurosci. 2007; 27:10350–10364. [PubMed: 17898207]

Lang T, Wacker I, Steyer J, Kaether C, Wunderlich I, Soldati T, Gerdes HH, Almers W. Ca2+-triggered peptide secretion in single cells imaged with green fluorescent protein and evanescent-wave microscopy. Neuron. 1997; 18:857–863. [PubMed: 9208853]

Lessmann V, Gottmann K, Heumann R. BDNF and NT-4/5 enhance glutamatergic synaptic transmission in cultured hippocampal neurones. Neuroreport. 1994; 6:21–25. [PubMed: 7703418]

Levine ES, Dreyfus CF, Black IB, Plummer MR. Brain-derived neurotrophic factor rapidly enhances synaptic transmission in hippocampal neurons via postsynaptic tyrosine kinase receptors. Proc. Natl. Acad. Sci. U. S. A. 1995; 92:8074–8077. [PubMed: 7644540]

Li YX, Zhang Y, Lester HA, Schuman EM, Davidson N. Enhancement of neurotransmitter release induced by brain-derived neurotrophic factor in cultured hippocampal neurons. J. Neurosci. 1998; 18:10231–10240. [PubMed: 9852560]

Lochner JE, Honigman LS, Grant WF, Gessford SK, Hansen AB, Silverman MA, Scalettar BA. Activity-dependent release of tissue plasminogen activator from the dendritic spines of hippocampal neurons revealed by live-cell imaging. J Neurobiol. 2006; 66:564–577. [PubMed: 16555239]

Lochner JE, Kingma M, Kuhn S, Meliza CD, Cutler B, Scalettar BA. Real-time imaging of the axonal transport of granules containing a tissue plasminogen activator/green fluorescent protein hybrid. Mol Biol Cell. 1998; 9:2463–2476. [PubMed: 9725906]

Lu B, Pang PT, Woo NH. The yin and yang of neurotrophin action. Nat Rev Neurosci. 2005; 6:603–614. [PubMed: 16062169]

Massey PV, Bashir ZI. Long-term depression: multiple forms and implications for brain function. Trends Neurosci. 2007; 30:176–184. [PubMed: 17335914]

Matsuoka Y, Kitamura Y, Taniguchi T. Induction of plasminogen in rat hippocampal pyramidal neurons by kainic acid. Neurosci Lett. 1998; 252:119–122. [PubMed: 9756336]

Mena MA, Treynor TP, Mayo SL, Daugherty PS. Blue fluorescent proteins with enhanced brightness and photostability from a structurally targeted library. Nat Biotechnol. 2006; 24:1569–1571. [PubMed: 17115054]

Mowla SJ, Farhadi HF, Pareek S, Atwal JK, Morris SJ, Seidah NG, Murphy RA. Biosynthesis and post-translational processing of the precursor to brain-derived neurotrophic factor. J Biol Chem. 2001; 276:12660–12666. [PubMed: 11152678]

Mowla SJ, Pareek S, Farhadi HF, Petrecca K, Fawcett JP, Seidah NG, Morris SJ, Sossin WS, Murphy RA. Differential sorting of nerve growth factor and brain-derived neurotrophic factor in hippocampal neurons. J Neurosci. 1999; 19:2069–2080. [PubMed: 10066260]

Ng YK, Lu X, Gulacsi A, Han W, Saxton MJ, Levitan ES. Unexpected mobility variation among individual secretory vesicles produces an apparent refractory neuropeptide pool. Biophys J. 2003; 84:4127–4134. [PubMed: 12770915]

Ohki EC, Tilkins ML, Ciccarone VC, Price PJ. Improving the transfection efficiency of post-mitotic neurons. J Neurosci Methods. 2001; 112:95–99. [PubMed: 11716945]

Pang PT, Teng HK, Zaitsev E, Woo NT, Sakata K, Zhen S, Teng KK, Yung WH, Hempstead BL, Lu B. Cleavage of proBDNF by tPA/plasmin is essential for long-term hippocampal plasticity. Science. 2004; 306:487–491. [PubMed: 15486301]

Perrais D, Kleppe IC, Taraska JW, Almers W. Recapture after exocytosis causes differential retention of protein in granules of bovine chromaffin cells. J Physiol. 2004; 560:413–428. [PubMed: 15297569]

Raymond CR. LTP forms 1, 2 and 3: different mechanisms for the “long” in long-term potentiation. Trends Neurosci. 2007; 30:167–175. [PubMed: 17292975]

Rosa P, Hille A, Lee RW, Zanini A, De Camilli P, Huttner WB. Secretogranins I and II: two tyrosine-sulfated secretory proteins common to a variety of cells secreting peptides by the regulated pathway. J Cell Biol. 1985; 101:1999–2011. [PubMed: 4055903]

Ryan TA. Kiss-and-run, fuse-pinch-and-linger, fuse-and-collapse: the life and times of a neurosecretory granule. Proc Natl Acad Sci U S A. 2003; 100:2171–2173. [PubMed: 12606723]

Salles FJ, Strickland S. Localization and regulation of the tissue plasminogen activator-plasmin system in the hippocampus. J Neurosci. 2002; 22:2125–2134. [PubMed: 11896152]

Saxton MJ, Jacobson K. Single-particle tracking: applications to membrane dynamics. Annu. Rev. Biophys. Biomol. Struct. 1997; 26:373–399. [PubMed: 9241424]

Scalettar BA. How neurosecretory vesicles release their cargo. The Neuroscientist. 2006; 12:164–176. [PubMed: 16514013]

Scalettar BA, Swedlow JR, Sedat JW, Agard DA. Dispersion, aberration and deconvolution in multi-wavelength fluorescence images. J Microsc. 1996; 182:50–60. [PubMed: 8632447]

Schwarzer C, Marksteiner J, Kroesen S, Kohl C, Sperk G, Winkler H. Secretoneurin: a market in rat hippocampal pathways. J Comp Neurol. 1997; 377:29–40. [PubMed: 8986870]

Sharma K, Fong DK, Craig AM. Postsynaptic protein mobility in dendritic spines: long-term regulation by synaptic NMDA receptor activation. Mol Cell Neurosci. 2006; 31:702–712. [PubMed: 16504537]

Shin CY, Kundel M, Wells DG. Rapid, activity-induced increase in tissue plasminogen activator is mediated by metabotropic glutamate receptor-dependent mRNA translation. J Neurosci. 2004; 24:9425–9433. [PubMed: 15496678]

Silverman MA, Johnson S, Gurkins D, Farmer M, Lochner JE, Rosa P, Scalettar BA. Mechanisms of transport and exocytosis of dense-core granules containing tissue plasminogen activator in developing hippocampal neurons. J Neurosci. 2005; 25:3095–3106. [PubMed: 15788766]

Swanwick CC, Harrison MB, Kapur J. Synaptic and extrasynaptic localization of brain-derived neurotrophic factor and the tyrosine kinase B receptor in cultured hippocampal neurons. J Comp Neurol. 2004; 478:405–417. [PubMed: 15384067]

Taraska JW, Perrais D, Ohara-Imaizumi M, Nagamatsu S, Almers W. Secretory granules are recaptured largely intact after stimulated exocytosis in cultured endocrine cells. Proc Natl Acad Sci U S A. 2003; 100:2070–2075. [PubMed: 12538853]

Teesalu T, Kulla A, Asser T, Koskiniemi M, Vaheri A. Tissue plasminogen activator as a key effector in neurobiology and neuropathology. Biochem Soc Trans. 2002; 30:183–189. [PubMed: 12023848]

Tsirka SE, Rogove AD, Bugge TH, Degen JL, Strickland S. An extracellular proteolytic cascade promotes neuronal degeneration in the mouse hippocampus. J Neurosci. 1997; 17:543–552. [PubMed: 8987777]

Tyler WJ, Pozzo-Miller L. Miniature synaptic transmission and BDNF modulate dendritic spine growth and form in rat CA1 neurones. J. Physiol. 2003; 553:497–509. [PubMed: 14500767]

Tyler WJ, Pozzo-Miller LD. BDNF enhances quantal neurotransmitter release and increases the number of docked vesicles at the active zones of hippocampal excitatory synapses. J. Neurosci. 2001; 21:4249–4258. [PubMed: 11404410]

Woo NH, Teng HK, Siao CJ, Chiaruttini C, Pang PT, Milner TA, Hempstead BL, Lu B. Activation of p75NTR by proBDNF facilitates hippocampal long-term depression. Nat Neurosci. 2005; 8:1069–1077. [PubMed: 16025106]

Wu LG. Kinetic regulation of vesicle endocytosis at synapses. Trends Neurosci. 2004; 27:548–554. [PubMed: 15331237]

Zagrebelsky M, Holz A, Dechant G, Barde YA, Bonhoeffer T, Korte M. The p75 neurotrophin receptor negatively modulates dendrite complexity and spine density in hippocampal neurons. J Neurosci. 2005; 25:9989–9999. [PubMed: 16251447]

Zhuo M, Holtzman DM, Li Y, Osaka H, DeMaro J, Jacquin M, Bu G. Role of tissue plasminogen activator receptor LRP in hippocampal long-term potentiation. J Neurosci. 2000; 20:542–549. [PubMed: 10632583]

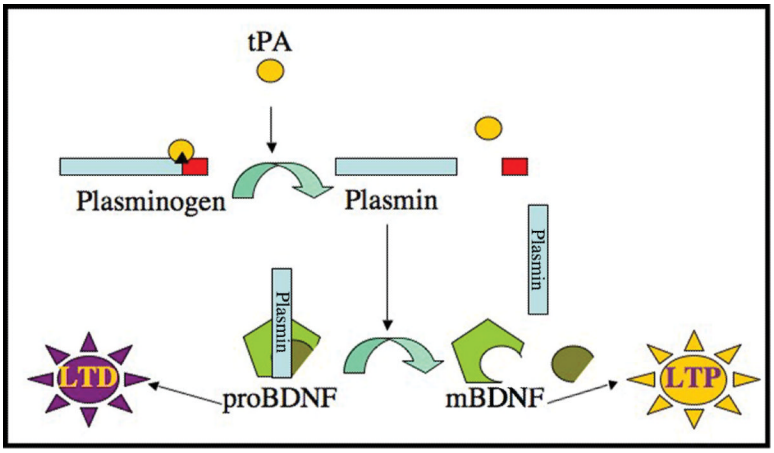

Figure 1. Hypothesized mechanism of tPA-modulated induction of long-term potentiation

tPA is a serine protease with substrate specificity for plasminogen. tPA-mediated conversion of plasminogen into the active protease plasmin facilitates the cleavage of proBDNF into mBDNF. proBDNF and mBDNF are hypothesized to induce opposing effects on synaptic communication. proBDNF elicits the weakening of synaptic connections associated with LTD, whereas mBDNF induces the strengthening of synaptic connections associated with LTP.

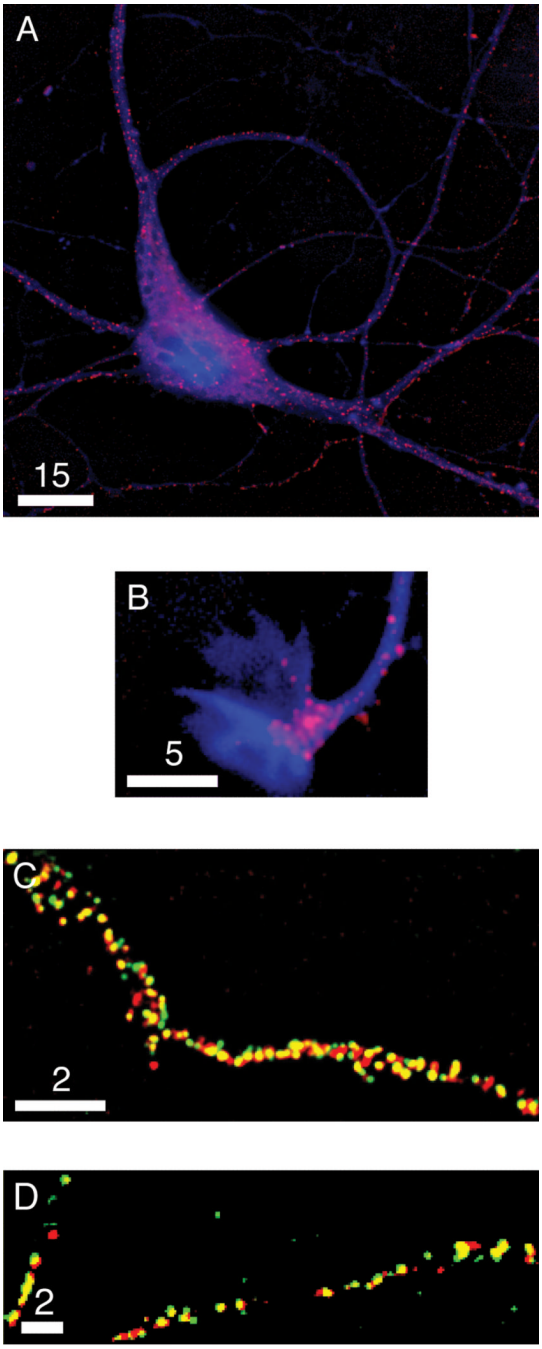

Figure 2. Plasminogen-mCherry is housed in DCGs

Deblurred fluorescence images of (A) the soma and processes of a fixed 7-DIV hippocampal neuron expressing plasminogen-mCherry (red) and Azurite (blue), (B) a growth cone of another fixed 7-DIV hippocampal neuron expressing these same two proteins, (C) a sub-region of a process of a fixed 4-DIV hippocampal neuron expressing plasminogen-mCherry (red) and proBDNF-EGFP (green), and (D) sub-regions of processes of a fixed 2-DIV hippocampal neuron expressing plasminogen-mCherry (red) and tPA-EGFP (green). Areas of overlap appear yellow. Bars = 15, 5, and 2 μm.

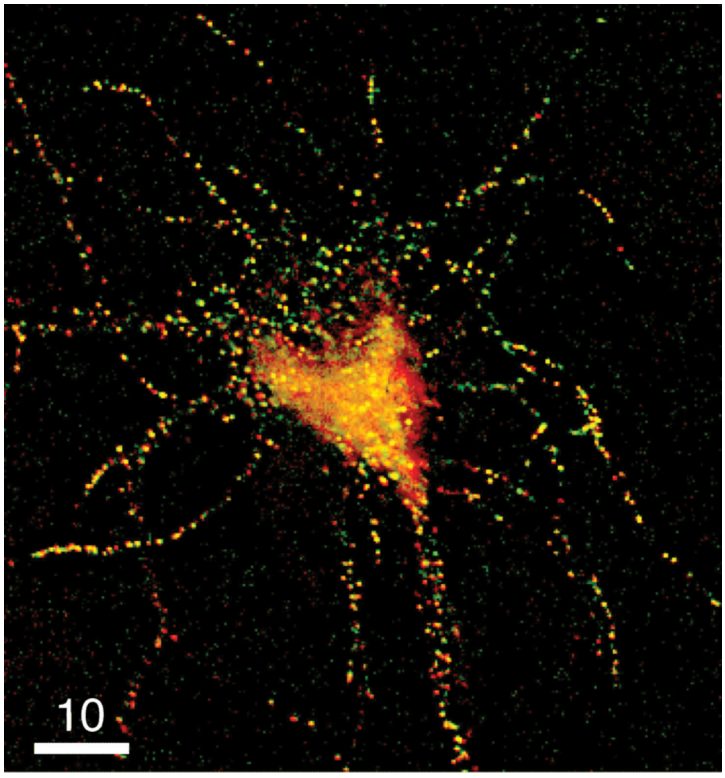

Figure 3. proBDNF-mCherry and tPA-EGFP are extensively co-packaged in DCGs

Deblurred fluorescence image of the soma and proximal processes of a fixed 8-DIV hippocampal neuron expressing tPA-EGFP (green) and proBDNF-mCherry (red). Areas of strong overlap appear yellow. Bar = 10 μm.

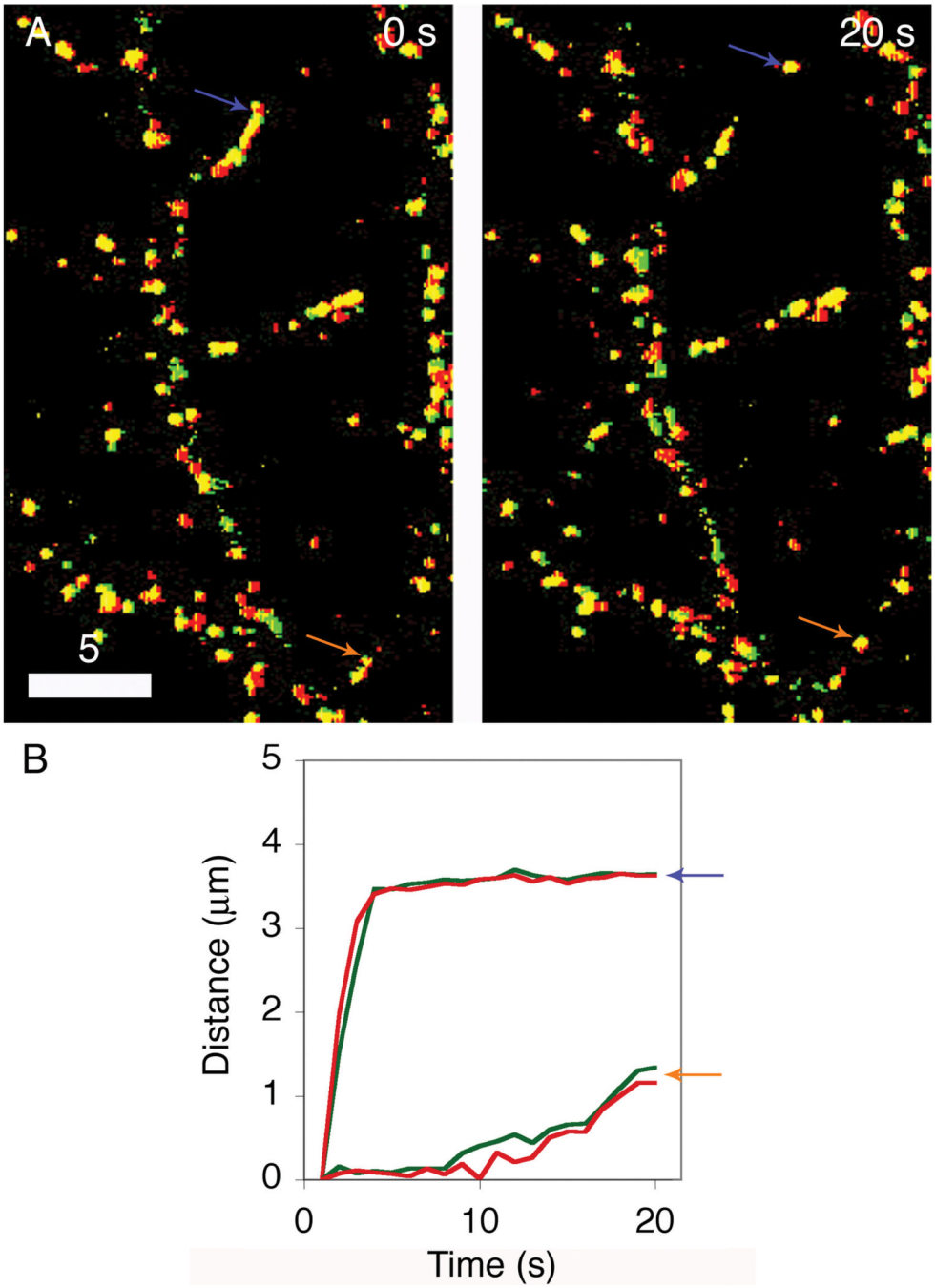

Figure 4. Neuromodulators are extensively co-packaged and co-transported in DCGs of living neurons

Fluorescence images (A) of the processes of a living 18-DIV hippocampal neuron expressing tPA-EGFP (green) and proBDNF-mCherry (red). The two pairs of colored arrows indicate corresponding positions of more slowly moving DCGs in time-lapse images separated by 20 s. Areas of overlap appear yellow. Plots of distance versus time (B) deduced by tracking the EGFP signals (green lines) and the mCherry signals (red lines) from the two DCGs in Panel A. Bar = 5 µm.

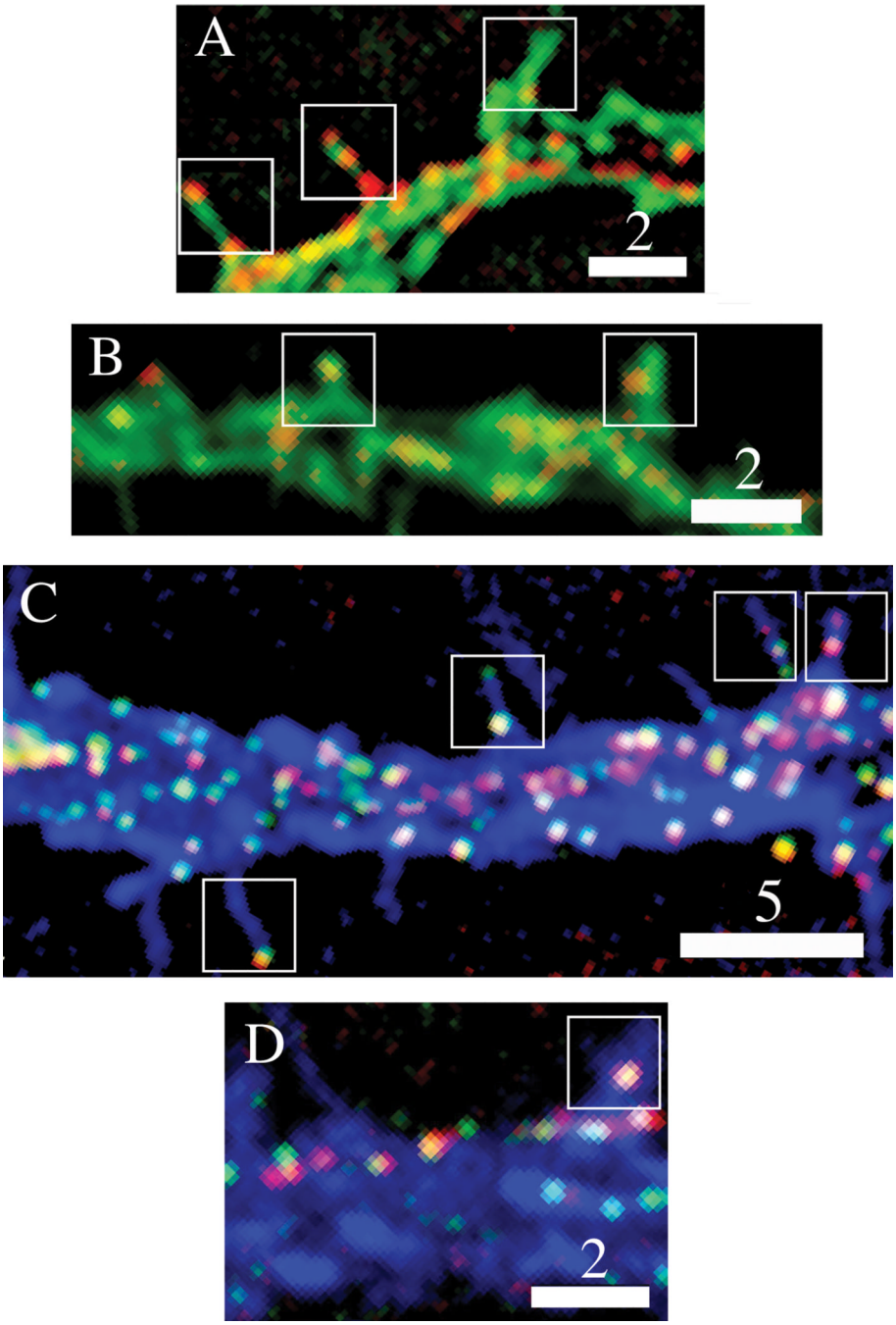

Figure 5. Neuromodulators localize to, and co-localize in, DCGs present in dendritic spines

Dual-color images showing (A) that proBDNF chimeras localize to DCGs in spines (boxes) of a fixed 15-DIV hippocampal neuron, and (B) that plasminogen chimeras localize to spines of a fixed 18-DIV neuron. Tri-color images showing (C) that DCGs containing both tPA (green) and proBDNF (red) chimeras localize to spines and an associated dendritic process (blue) of a fixed 16-DIV hippocampal neuron, and (D) that DCGs containing both plasminogen (red) and proBDNF (green) chimeras localize to spines and the associated dendritic process of a fixed 15-DIV neuron. Bars = 2 and 5 μm.

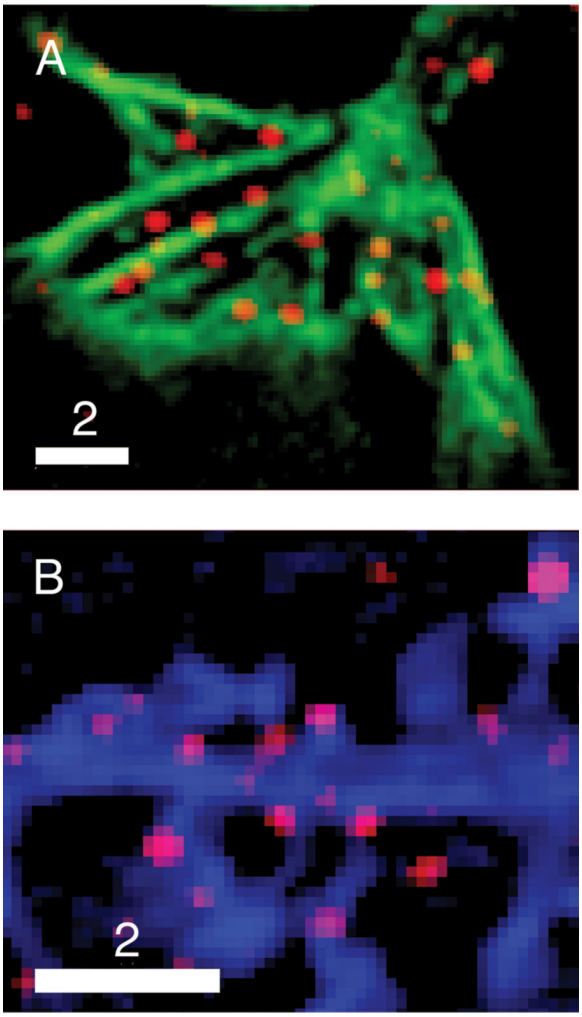

Figure 6. Expression patterns of chimeric and endogenous neuromodulators are similar

Dual-color images showing that puncta stained by an antibody against endogenous proBDNF (A) are present in the growth cone of a fixed 5-DIV hippocampal neuron stained with FITC-phalloidin, and (B) are present in spines and part of a process from a fixed 17-DIV hippocampal neuron expressing Azurite. Bars = 2 μm.

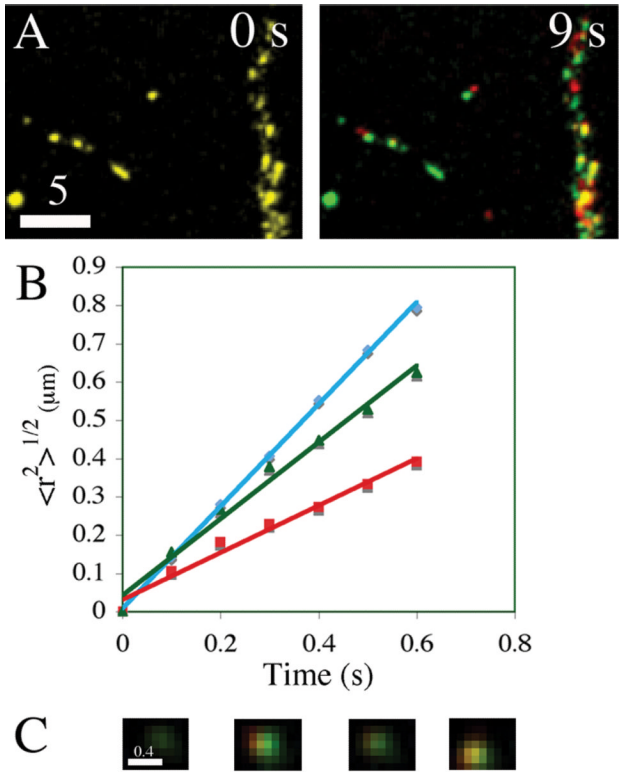

Figure 7. A pool of rapidly mobile DCGs containing neuromodulators is present near sites of release

Dual-color images (A) showing that the distribution of DCGs containing tPA and proBDNF chimeras changes appreciably over the time scale of < 9 s. In these images, green denotes DCG positions at a fixed initial time, red denotes DCG positions at the specified later time, and yellow denotes overlap of green and red. After 9 s, overlap (yellow), which reveals immobility, is significantly lost.

Plots of $\langle r^2 \rangle^{1/2}$ versus t (B) deduced from trajectories of DCGs in Panel A. These plots are linear, implying that the DCG trafficking was directed, and their slopes give speeds on the order of one μm/s, revealing that trafficking was rapid.

Dual-color TIRFM images (C) showing a membrane-proximal DCG containing tPA and proBDNF chimeras undergoing intensity flicker as it changes depth in the evanescent field. Bars = 5 and 0.4 μm.